Neuron 48, 689–701, February 15, 2005 ©2005 Elsevier Inc. DOI 10.1016/j.neuron.2005.10.022

Bone Marrow-Derived Microglia Play a Critical Role in Restricting Senile Plaque Formation in Alzheimer's Disease

Alain R. Simard,[1] Denis Soulet,[1] Genevieve Gowing,[1] Jean-Pierre Julien,[1] and Serge Rivest[1,*]
[1] Laboratory of Molecular Endocrinology
CHUL Research Center and
Department of Anatomy and Physiology
Laval University
2705 Laurier boul.
Québec G1V 4G2
Canada

Summary

Microglia are the immune cells of the brain. Here we show a massive infiltration of highly ramified and elongated microglia within the core of amyloid plaques in transgenic mouse models of Alzheimer's disease (AD). Many of these cells originate from the bone marrow, and the β-amyloid-40 and -42 isoforms are able to trigger this chemoattraction. These newly recruited cells also exhibit a specific immune reaction to both exogenous and endogenous β-amyloid in the brain. Creation of a new AD transgenic mouse that expresses the thymidine kinase protein under the control of the CD11b promoter allowed us to show that blood-derived microglia and not their resident counterparts have the ability to eliminate amyloid deposits by a cell-specific phagocytic mechanism. These bone marrow-derived microglia are thus very efficient in restricting amyloid deposits. Therapeutic strategies aiming to improve their recruitment could potentially lead to a new powerful tool for the elimination of toxic senile plaques.

Introduction

Alzheimer's disease (AD) is the most prevalent cause of dementia in humans, and the symptoms are generally manifested after the seventh decade of life. Unfortunately, the causes of the disease remain largely unknown, and this limits the development of therapeutic strategies to treat the disease. It is a well-accepted fact that deposition of aggregated β-amyloid to form amyloid plaques (also known as senile plaques) is the hallmark of AD. It is therefore important to study the development of these deposits, as well as the effects they have on their cellular environment. Many studies have provided evidence that microglia are attracted to and surround senile plaques both in human samples and in rodent transgenic models that develop this disease (Dickson et al., 1988; Haga et al., 1989; Itagaki et al., 1989; Perlmutter et al., 1992; Sheng et al., 1997; Frautschy et al., 1998; Wegiel et al., 2001, 2003, 2004; Malm et al., 2005).

The precise role of these cells is still under debate. A first proposal is that these microglia become activated in the presence of β-amyloid and secrete neurotoxic molecules, whereas they may also have a neuroprotective function by secreting neurotrophic agents and eliminating β-amyloid via phagocytosis. In support of the neurotoxic hypothesis, a few in vitro studies of cultured primary microglial cells have demonstrated that they secrete high levels of cytokines when stimulated with β-amyloid peptides (Kim and de Vellis, 2005; Walker and Lue, 2005). This has been linked to cytokine production and neuronal death in cell cultures (Giulian et al., 1996; Walker and Lue, 2005). Moreover, initial clinical trials involving the treatment of patients with nonsteroidal anti-inflammatory drugs (NSAIDs) prior to the onset of AD have suggested that inhibiting the immune response reduces the occurrence of the disease (Stewart et al., 1997; Anthony et al., 2000; in t' Veld et al., 2001; Yip et al., 2005). Microglia are also believed to be unable to infiltrate the plaques and eliminate β-amyloid deposits by phagocytosis (Wegiel et al., 2001, 2003, 2004). These data have lead to the assumption that the brain's resident macrophages promote the development of the disease, since they produce cytotoxic elements and are unable to clear the β-amyloid deposits.

On the other hand, many studies support the idea that microglia are beneficial to the diseased brain. Indeed, activated microglia are known to favor the release of many neurotrophic molecules that have clear beneficial properties for CNS elements, including neurons and oligodendrocytes (Nguyen et al., 2002). In this regard, microglia inhibition causes extensive damage in acute models of neurotoxicity (Turrin and Rivest, 2006). In addition, it has been demonstrated that an immune response in the CNS reduces amyloid deposition (Rogers et al., 2002; Malm et al., 2005). Some also argue that NSAIDs have no effect in patients suspected to have already developed AD (Aisen et al., 2003) and that treatment with a cyclooxygenase-2 inhibitor increases the amount of β-amyloid found in the brain (Kukar et al., 2005). Moreover, the notion that microglia are able to phagocytose amyloid deposits has been supported in previous reports (Rogers and Lue, 2001; Rogers et al., 2002; Liu et al., 2005). It is thus crucial to further elaborate the role of microglia in the etiology of AD.

We and others have recently demonstrated that bone marrow-derived cells are able to cross the blood-brain barrier (BBB) and differentiate into fully functional microglia (Hess et al., 2004; Simard and Rivest, 2004a; Malm et al., 2005). We also demonstrated that newly differentiated blood-derived microglia express higher levels of proteins that are required for antigen presentation and may thus be more efficient phagocytes than resident microglia (Simard and Rivest, 2004a). In light of this, we examined the origin of microglial cells that are associated with senile plaques in a rodent transgenic animal that harbors a mutant human presenilin 1 and a chimeric mouse/human β-amyloid precursor protein (APP_{Swe}). These animals develop amyloid deposits similar to those found in brains of humans diagnosed with AD. We found that a large portion of the plaque-associated microglia were of blood origin. These cells are specifically attracted to β-amyloid-40/42, the most prevalent

*Correspondence: serge.rivest@crchul.ulaval.ca

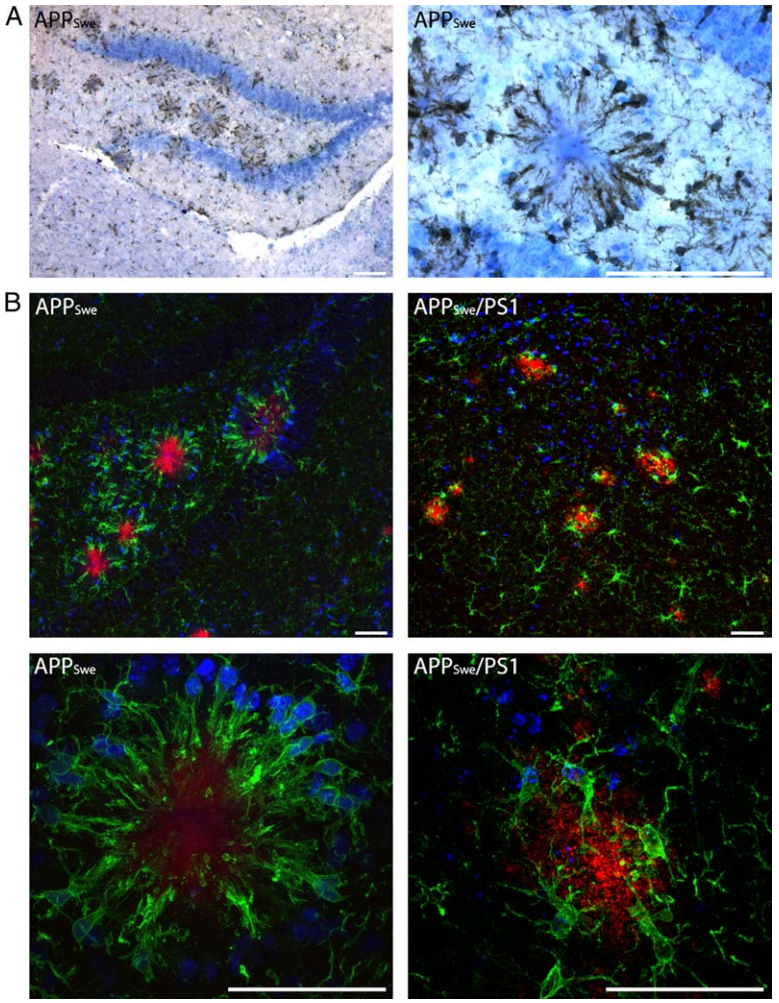

Figure 1. Microglial Cells Infiltrate Amyloid Plaques in APP_{Swe} and APP_{Swe}/PS1 Transgenic Animals

(A) Microglial cells in brain tissue sections taken from APP_{Swe} mice were stained with an anti-*iba1* antibody and peroxidase-conjugated secondary antibody, which were then developed with DAB solution (brown elongated cells). Tissues were also stained with thionine. Note the particular ring formation of microglial cells surrounding the amyloid core (blue staining in the center of microglial ring). (B) To compare amyloid plaques and microglial cell localization between the APP_{Swe} (15-month-old) and APP_{Swe}/PS1 (9-month-old) transgenic animals, tissue sections were stained with Congo red or with an anti-β-amyloid-42 antibody to reveal amyloid plaques (red), DAPI to visualize cell nuclei (blue), and anti-*iba1* primary antibody/Alexa 488-conjugated secondary antibody to reveal microglial cells (green). Note that microglial cells surround and their projections infiltrate senile plaques in both transgenic models for AD. Scale bars represent 50 μm.

and toxic β-amyloid isoforms found in the human brain. We also show that these animals do not respond to this protein with a classical innate immune response frequently observed in acute models of neurotoxicity. More importantly, we demonstrate that bone marrow-derived microglia eliminate amyloid deposits, since transgenic animals that specifically fail to recruit these cells to the CNS had more plaques than their control littermates. According to our results, bone marrow-derived microglia reduce the amyloid deposits via phagocytosis of β-amyloid and thus play a critical role by restricting AD progression. These findings present important information that could lead to the development of a new and effective therapy for the treatment of this devastating disease.

Results

Microglial Cells Infiltrate Amyloid Deposits in Rodent Models of AD

It is known that many microglial cells surround senile plaques in humans (Dickson et al., 1988; Haga et al., 1989; Itagaki et al., 1989) and in rodent transgenic animals that develop amyloid deposits (Perlmutter et al., 1992; Sheng et al., 1997; Frautschy et al., 1998; Wegiel et al., 2001, 2003). In order to test whether similar results would be obtained in the double-mutant transgenic line used in this study, we compared the localization of microglia near senile plaques from the APP_{Swe}/PS1 mutant transgenic line with those of the more characterized APP_{Swe} single-mutant line. As shown in Figure 1, amyloid plaques are completely surrounded by microglial cells in both transgenic lines, demonstrating that both models share the same characteristics. Interestingly, we have observed that ramifications of microglial cells appear to infiltrate the core of amyloid plaques (see Figure 1 and Movie S1). There seems to be a chemoattractant gradient from the center of the plaques, and this phenomenon was not necessarily dependent on the volume or the location of the plaques. Although both mouse lines exhibited a tight association between β-amyloid and microglia, APP_{Swe} single-mutant mice take 12–15 months to develop plaques, while this process is much faster in the brain of APP_{Swe}/PS1 mutant mice (see below).

Age-Related Migration of Blood-Derived Cells toward Amyloid Plaques

A recent study suggests that resident microglia are less immunocompetent than their blood-derived counterparts (Simard and Rivest, 2004a). Based on these results and the fact that highly ramified and elongated microglia

penetrate the core of the plaques, we tested whether these cells were resident or blood-derived microglia. To this end, we irradiated 2-month-old APP_{Swe}/PS1 mutant transgenic mice and transplanted GFP-expressing bone marrow cells into their blood streams. We then sacrificed the animals 2–7 months later and observed brain tissue samples from these mice. It became clear to us that a large percentage of the amyloid plaque-associated microglia were GFP positive, demonstrating that many of these cells originate from the blood (Figures 2A and 2B). Of interest, there is also an age-associated increase in the amount of infiltrating cells up to the age of 6 months, whereas their number slightly decreased around 9 months of age. We thus quantitatively measured the amount of plaques present in the hippocampus and cortex of these animals, along with their size and the amount of GFP-positive microglia associated with the amyloid deposits (Figure 2C). The values obtained for the number of plaques in the combined sample areas of each animal were 9.4 ± 2.1 (number of plaques ± SEM), 6.0 ± 2.2, 48.4 ± 3.3, and 91.0 ± 25.0 plaques for 4 (n = 5), 5 (n = 5), 6 (n = 5), and 9 (n = 2) month-old mice, respectively. One-way ANOVA analysis showed a statistical difference between the groups ($f_{(3,13)} = 36.97$, $p < 0.001$), demonstrating that the number of plaques significantly increased with the age of the animal. A similar phenomenon was observed regarding the size of the plaques, which had mean areas of 124.4 ± 5.4 μm^2 (mean area ± SEM), 152.5 ± 20.0 μm^2, 192.8 ± 16.1 μm^2, and 389.2 ± 7.8 μm^2 in the same age groups, respectively ($f_{(3,13)} = 33.49$, $p < 0.001$). Moreover, we found that plaques present in 4- and 5-month-old mice had 0.20 ± 0.10 (number of microglia ± SEM) and 0.12 ± 0.10 plaque-associated GFP^+ microglia, whereas the number significantly increased to 0.94 ± 0.18 ($p < 0.01$) at 6 months of age. Interestingly, the amount of GFP-positive microglial cells associated to the amyloid plaques slightly diminished after 9 months of age (0.67 ± 0.17), although the difference with the other age groups was not statistically significant. These data demonstrate that blood-derived cells infiltrate the brain and migrate toward amyloid plaques throughout the development of the disease and that blood-derived microglial migration toward the amyloid deposits generally seems to occur after the plaques have achieved a certain size rather than prior to their formation.

β-Amyloid Peptides Recruit and Activate Blood-Derived Microglial Cells

The signal that triggers the infiltration of blood-derived microglia in this model of AD has yet to be unravelled. Moreover, the ability of different β-amyloid isoforms to specifically recruit and activate microglial cells in vivo is still under debate. We thus generated chimeric mice by transplanting GFP-expressing bone marrow cells into irradiated wild-type mice. Three months later, we injected 1 μl of either saline, β-amyloid-31, β-amyloid-40, β-amyloid-42, or β-amyloid-57 (1 μg/μL for each peptide) directly into the hippocampus of these animals. The animals were sacrificed 3–7 days following the injection, and cross-sections of the hippocampus were examined for the presence of GFP-positive cells. As shown in Figure 3A, β-amyloid-40 and β-amyloid-42 isoforms were able to provoke the infiltration of GFP-positive cells even in areas distal to the injection site. These results suggest that bone marrow-derived microglia are specifically attracted to the β-amyloid-40/42 isoforms.

We next tested whether microglia were immunologically activated by β-amyloid-42. To achieve this goal, we injected β-amyloid-42 into the hippocampus of wild-type CD1 mice. Over the course of 72 hr after the injection, we studied the expression levels of many genes that are normally induced during an innate immune response, such as TLR2, TNF-α, IL-1β, and MCP-1 (Figures 3B and 3C). We found the expression of TLR2, IL-1β, and MCP-1 mRNAs to be greatly increased following β-amyloid-42 treatment when compared to their saline-treated littermates. Conversely, the hybridization signal for TNF-α remained undetectable in the brain of acutely treated mice throughout the 3 day period after the injection, suggesting that β-amyloid-42 does not elicit a typical innate immune response. Taken together, these data demonstrate that β-amyloid peptides commonly found in AD can recruit blood-derived microglia and induce an innate immune response in vivo, although this process does not involve the inflammatory molecule TNF-α.

We next determined whether a similar immune reaction takes place in the brains of APP_{Swe}/PS1 double-mutant transgenic mice. We thus examined whether the mRNA expression of the same genes in brain tissue sections of 4- to 9-month-old APP_{Swe}/PS1 mice was higher than in WT animals and whether it colocalized with amyloid plaques (Figures 4A and 4B). We found that TLR2- and IL-1β-expressing cells were localized in the vicinity of amyloid plaques and that their expression levels increased proportionally with the age of the animals, whereas the signal for TNF-α mRNA was not detectable in the CNS at all ages. MCP-1 expression in transgenic versus WT mice was comparable until the age of 6 months, whereas it greatly increased in the brains of 9-month-old APP_{Swe}/PS1 animals. Taken together, our data demonstrate that a similar and specific immune activity occurs in response to exogenous β-amyloid-42 administration and endogenous β-amyloid deposits.

Blood-Derived Microglia Reduce Amyloid Deposits

To this point, we have shown that many bone marrow-derived cells infiltrate the brain and are greatly attracted to β-amyloid deposits. However, the role of these cells in the development of senile plaques remains unclear. To establish whether blood-derived microglia are beneficial or detrimental to the development of AD, we crossed the APP_{Swe}/PS1 double-mutant transgenic mice with a new line of transgenic animals that express a mutant thymidine kinase (TK) protein under the control of the CD11b promoter. When treated with ganciclovir, all cells expressing the TK protein (those of monocytic lineage only) are eliminated when they undergo cellular division. However, these animals no longer produce macrophages, which are essential for the enucleation of red blood cells, and thus our mice died from anemia when treated with ganciclovir i.p. for a period of 10 days. Because we hypothesized that a longer treatment would be required to have a significant effect on amyloid plaque formation, we were compelled to deliver the drug by other means. We thus chose to deliver the drug directly into the CNS by installing a chronic in-dwelling

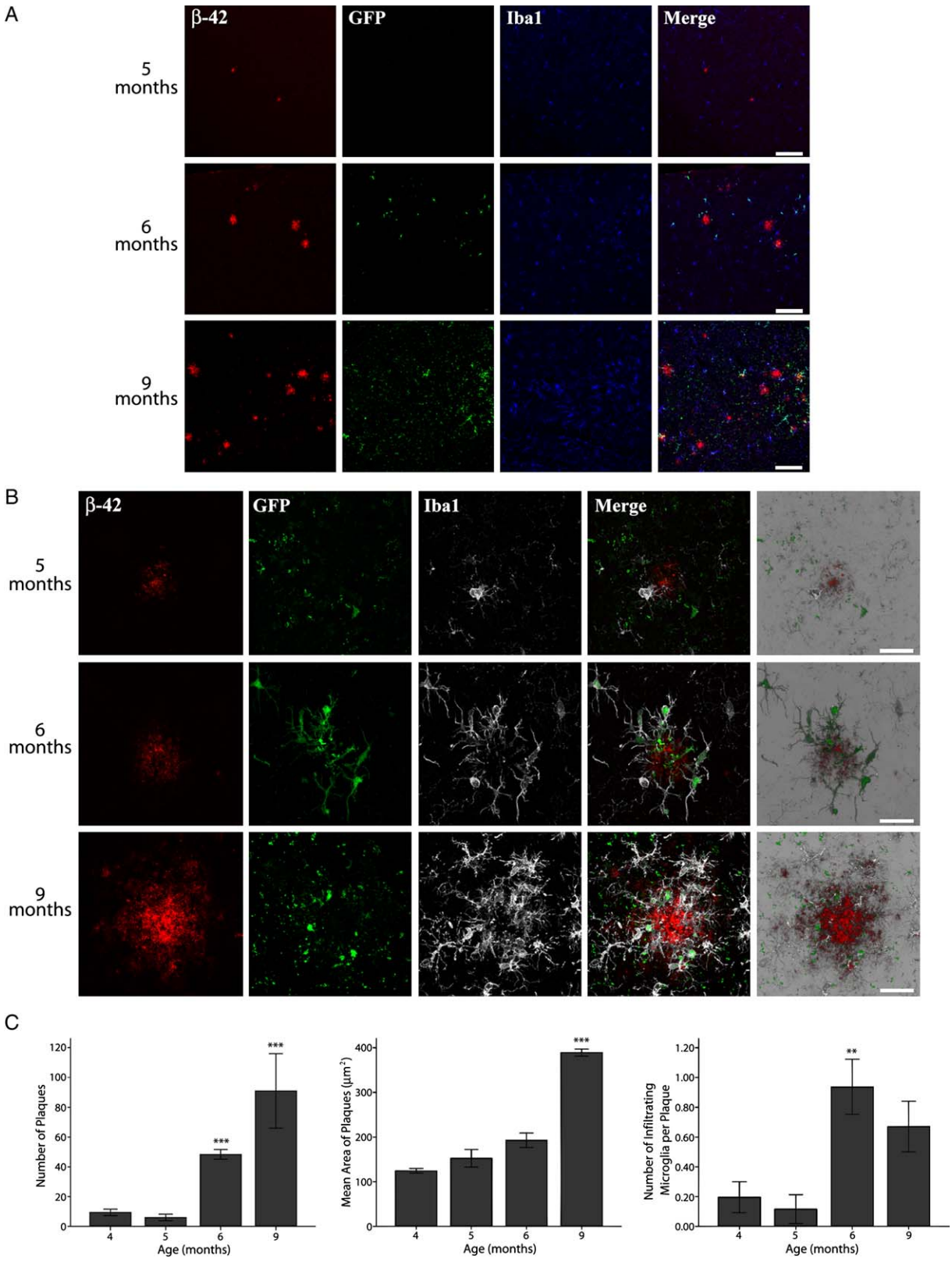

Figure 2. Microglia of Bone Marrow Origin Migrate toward Endogenous β-Amyloid

(A and B) Brain sections of 5-, 6-, and 9-month-old APP_{Swe}/PS1 mice harboring GFP-expressing cells in their bloodstream were immunohistochemically stained to reveal amyloid plaques (β-42 antibody), GFP-positive cells (GFP), and microglia (*iba1* antibody). A large portion of plaque-associated microglia expressed GFP, indicating that they originated from bone-marrow stem cells. In (B), colors were optimized to better visualize GFP and *iba1* colocalization (white background Merge). Scale bars represent 100 μm and 25 μm in (A) and (B), respectively. (C) The number and size of amyloid plaques as well as the number of plaque-associated GFP-positive microglial cells in 4-, 5-, 6-, and 9-month-old APP_{Swe}/PS1

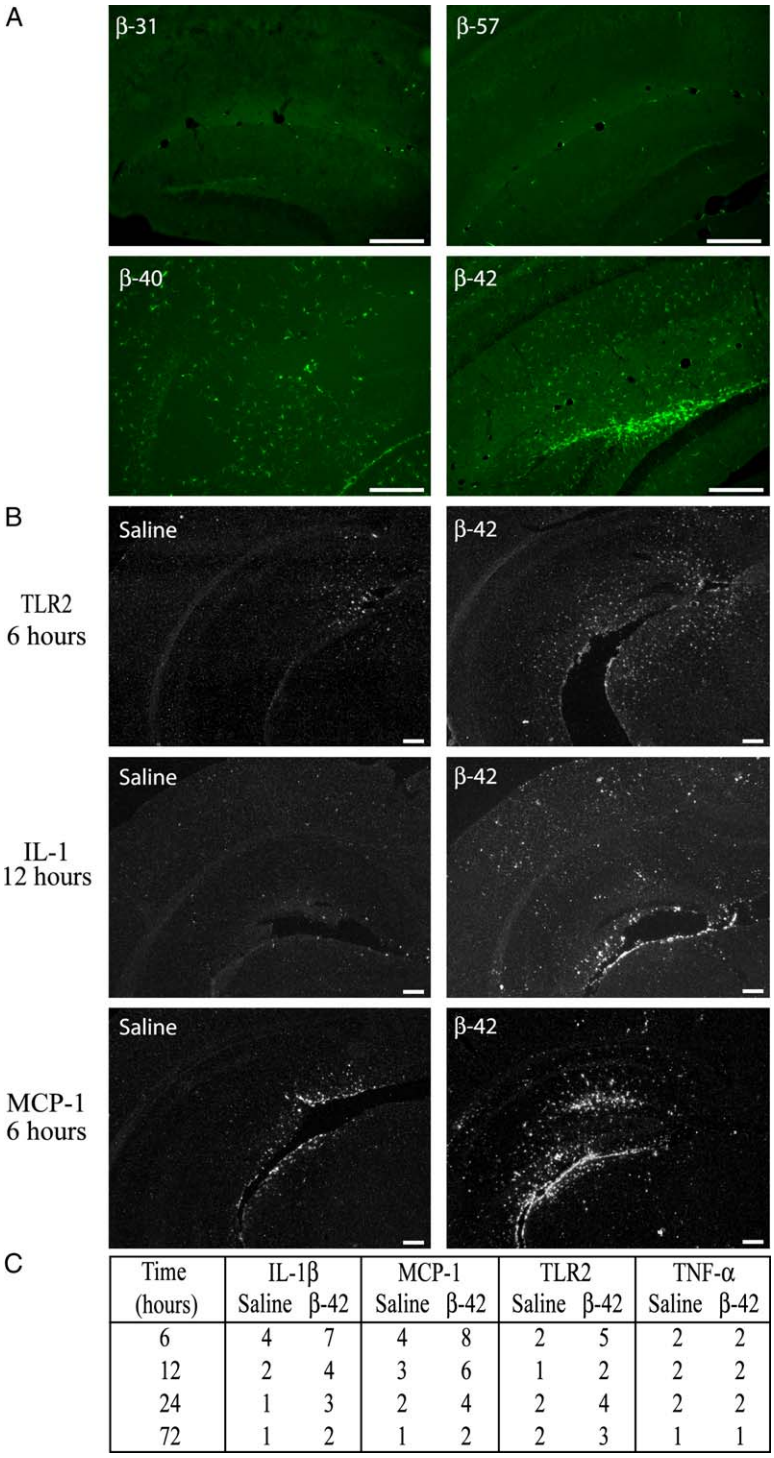

C

Time (hours)	IL-1β		MCP-1		TLR2		TNF-α	
	Saline	β-42	Saline	β-42	Saline	β-42	Saline	β-42
6	4	7	4	8	2	5	2	2
12	2	4	3	6	1	2	2	2
24	1	3	2	4	2	4	2	2
72	1	2	1	2	2	3	1	1

Figure 3. Exogenous β-Amyloid Induces the Infiltration of Blood-Derived Microglia into the CNS and Induces an Immune Response

(A) Four different β-amyloid isoforms (β-31, β-40, β-42, and β-57) or saline (not shown) were injected into the hippocampus of GFP-chimeric mice. Seven days later, GFP-positive microglia were found throughout the hippocampus of β-40- and β-42-treated animals, even in areas much distal to the injection site. Bone-derived microglia did not migrate into the CNS in response to the β-31 and β-57 isoforms. Scale bar represents 200 μm. (B) Saline or β-42 was injected in the same hippocampal area of CD1 mice, and mRNA expression of TLR2, IL-1, MCP-1 and TNF-α was visualized by in situ hybridization at different time points. The expression of TLR2, IL-1, and MCP-1 were found to be increased following acute β-42 treatment in areas distal to the injection site. Scale bar represents 250 μm. Photographs in (A) and (B) represent the general response observed in each group. (C) Qualitative mRNA expression analysis of the same four genes demonstrates that IL-1β, MCP-1, and TLR2 are upregulated between 6 and 72 hr post-β-42 treatment, whereas TNF-α transcript remained comparable to background levels.

cannula into the right lateral ventricle of 15- to 24-week-old APP_{Swe}/PS1 mice and connecting the cannula to an Alzet osmotic mini-pump that delivered the solution over a period of 28 days. With this method, we ensured that monocytes in the vicinity of the brain would be exposed to ganciclovir and eliminated prior to their differentiation into microglia (also see Figure S1), while systemic macrophages remain intact. In this regard, mice survived and did not show any particular signs of sickness during the chronic i.c.v. ganciclovir infusion.

Cross-sections of the brains were immunohistochemically stained for amyloid deposits and microglial

mice were quantitatively analyzed, and the means for each group are presented in these graphs. Error bars represent standard error of means. Three asterisks denote significant difference ($p < 0.05$) with all three other age groups, whereas the group with two asterisks is different from 4 and 5 month groups.

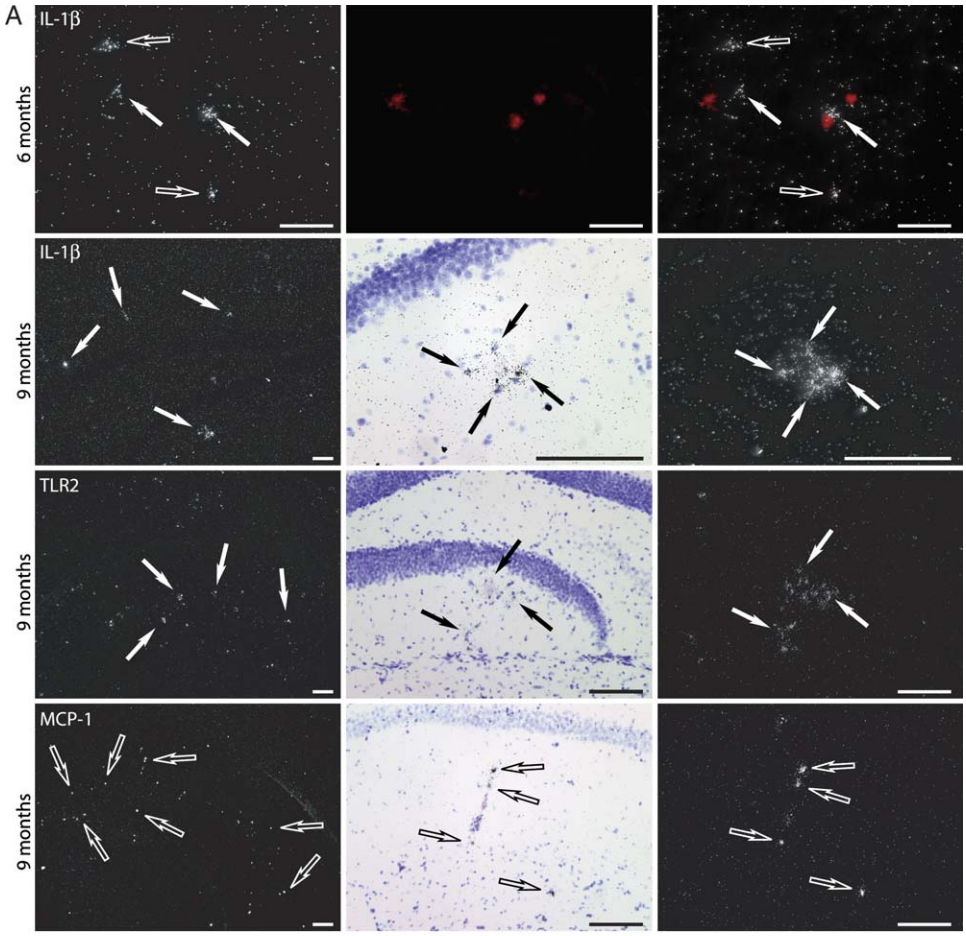

B

Age (months)	IL-1β	MCP-1	TLR2	TNF-α
4	2	2	2	2
5	3	2	3	2
6	5	2	4	2
9	6	6	8	--

Figure 4. Endogenous β-Amyloid also Activates Immune Cells

(A and B) mRNA expression of IL-1β, MCP-1, TLR2, and TNF-α was observed at different stages of plaque formation. (A) Dark (first and third columns) and bright (second column) field photomicrographs at low magnification (first column) or high magnification (second and third columns) are representative of general mRNA expression found in all animals of their respective age groups. (B) The table corresponds to a qualitative analysis of the expression of each gene at 4, 5, 6, and 9 months of age. Similarly to exogenous β-amyloid-42, the endogenous amyloid protein induces the expression of IL-1β, MCP-1, and TLR2 but not TNF-α. Note that MCP-1 expression was only increased in animals older than 6 months. Scale bars represent 100 μm.

cells (Figure 5A). We next quantified the number and size of the amyloid plaques as well as the number of plaque-associated microglia in saline- versus ganciclovir-treated animals (Figure 5B). As expected, the number of microglial cells in contact with amyloid deposits were not different between saline and ganciclovir groups ($f_{(2,27)}$ = 0.371, p = 0.694). However, the number of plaques in saline-treated animals were on average in the order of 23.3 ± 13.6 (n = 3), 30.0 ± 16.7 (n = 2), and 16.7 ± 13.6 (n = 3) in 4-, 5-, and 6-month-old animals, respectively. In animals treated with ganciclovir, there were 19.7 ± 7.5 (n = 10), 39.7 ± 7.9 (n = 8), and 69.8 ± 9.6 (n = 6) plaques in 4-, 5-, and 6-month old animal groups, respectively. A two-way ANOVA suggested that a slight interaction between saline and ganciclovir groups ($f_{(2,27)}$ = 3.286, p = 0.053) was present. After post-hoc considerations (Bonferroni t test) while assuming interaction between groups, the number of plaques in saline and ganciclovir treatments in the 6 month group were significantly different (p = 0.004). The mean areas of plaques in saline-treated animals were 264.0 ± 38.0 μm^2 (n = 3), 301.1 ± 46.6 μm^2 (n = 2), and 163.2 ± 38.0 μm^2 (n = 3) in 4-, 5-, and 6-month-old groups, respectively, whereas in ganciclovir-treated groups the mean areas of plaques were 178.1 ± 20.8 μm^2 (n = 10), 262.2 ± 22.0 μm^2 (n = 8), and 302.0 ± 26.9 μm^2 (n = 6) in the same respective age groups. The two-way ANOVA indicates a statistically significant interaction between

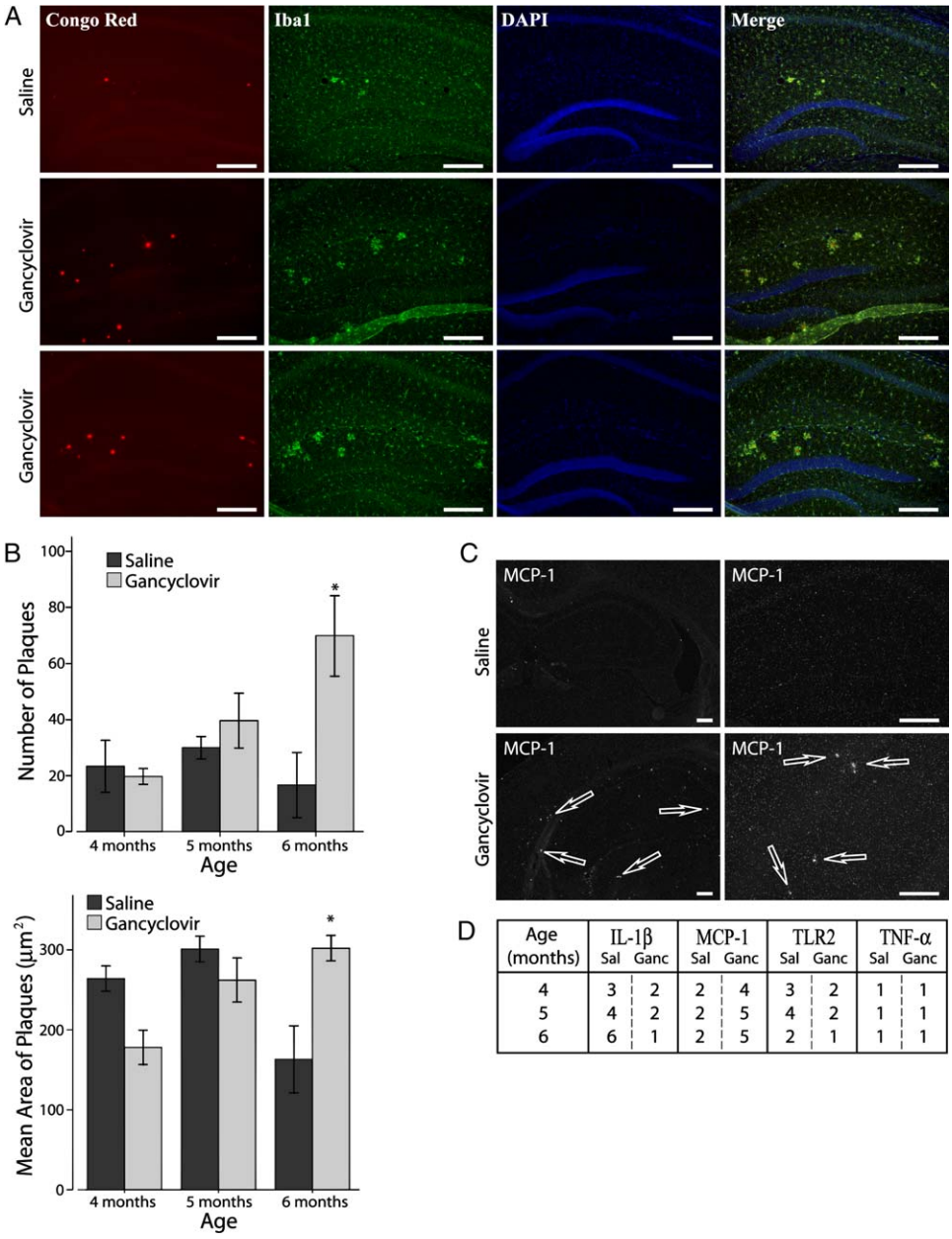

Age (months)	IL-1β Sal	IL-1β Ganc	MCP-1 Sal	MCP-1 Ganc	TLR2 Sal	TLR2 Ganc	TNF-α Sal	TNF-α Ganc
4	3	2	2	4	3	2	1	1
5	4	2	2	5	4	2	1	1
6	6	1	2	5	2	1	1	1

Figure 5. Bone Marrow-Derived Microglia Eliminate Amyloid Deposits In Vivo

Saline or ganciclovir was administered to APP-TK mice via an Alzet osmotic mini-pump attached to an indwelling cannula inserted into the right lateral ventricle for 28 days. (A) Tissues were then stained to reveal amyloid plaques (Congo red), microglia (*iba1* antibody) and nuclei (DAPI). Pictures indicate the general response seen in two different 6-month-old treated animals. (B) Stereological quantitative analysis of the number and size of plaques found in the cortex and hippocampus. The asterisks denote significant difference with the age-matched saline group. Error bars represent SEM. (C and D) Visual observations and qualitative analysis of gene expression reveals that IL-1β and TLR2 mRNAs were down-regulated following ganciclovir treatments, whereas MCP-1 expression was upregulated and TNF-α remained at constitutive levels. Scale bars in (A) and (C) represent 200 μm.

saline- and ganciclovir-treated groups ($f_{(2,27)} = 6.688$, $p = 0.004$). Bonferroni post-hoc tests demonstrated that the average size of plaques in saline and ganciclovir groups was significantly different only in 6-month-old animals ($p = 0.006$). In conclusion, these data suggest that blood-derived microglia play an important role in reducing the number and the size of amyloid plaques.

To verify that our treatment method had an effect on the immune response in these animals, we examined the expression levels of TLR2, IL-1β, MCP-1, and TNF-α by in situ hybridization. We found that IL-1β and TLR2 levels were lower in ganciclovir-treated animals compared to the saline-treated mice at all ages, whereas MCP-1 expression was more prevalent in the animals that received the drug (Figures 5C and 5D). On the other hand, TNF-α expression was still undetectable after ganciclovir treatment. These data suggest that our delivery method was effective at inhibiting a large part of the

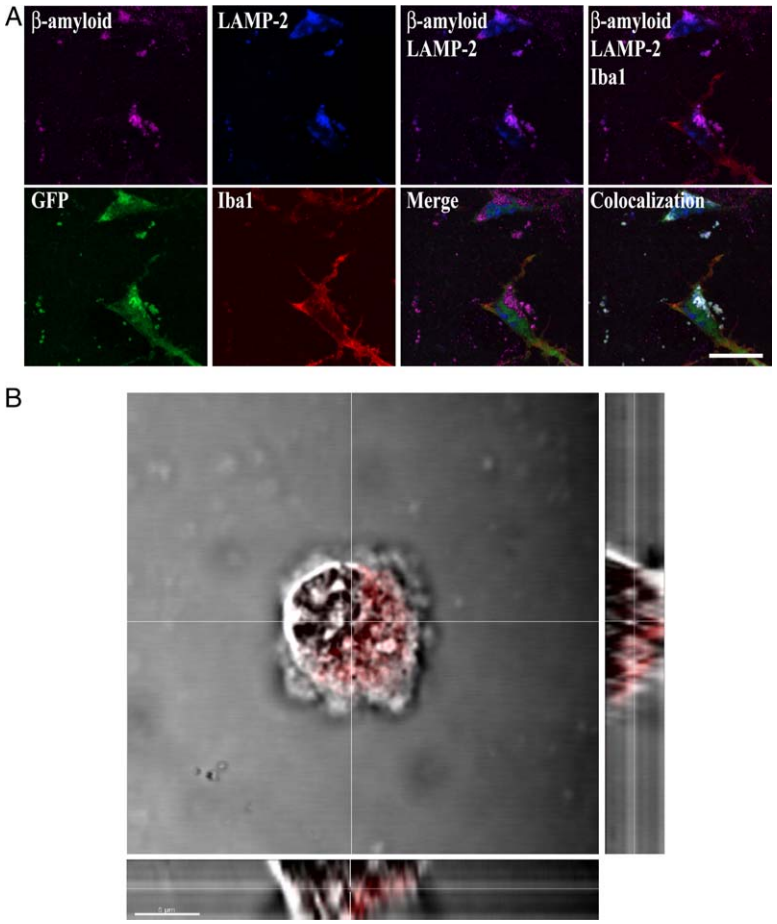

Figure 6. Microglia of Bone Marrow Origin Are Able to Clear β-Amyloid by Phagocytosis

(A) Six-month-old APP_{Swe}/PS1 tissues were immunohistochemically stained to reveal β-amyloid, lysosomes (LAMP-2), bone marrow-derived cells (GFP), and microglia (*iba1*). As seen in the merged photographs, β-amyloid colocalizes with lysosomes in GFP-positive microglia in vivo. Scale bar represents 10 μm. (B) BV2 microglial cells were treated with Cy3-conjugated β-$amyloid_{1-42}$ peptide and examined by confocal microscopy. It is evident that the β-amyloid peptide (red) was present inside the cell (white membrane), as demonstrated by the different planes of view. These data confirm that microglia are able to phagocytose β-amyloid. Scale bar represents 5 μm.

immune response normally associated with amyloid plaques, and this was most likely accomplished by preventing the infiltration of blood-derived microglia.

Phagocytosis of β-Amyloid by Blood-Derived Microglial Cells

While analyzing the different Congo red-stained tissues that were used in these studies, we often observed small β-amyloid deposits inside many microglial cells (see Movie S2). This initial result was confirmed with anti-β-amyloid-42 antibody-stained tissues that were observed by confocal microscopy. After reconstructing the images with 3D software, it became clear to us that small amyloid deposits were specifically detected within subcellular compartments of microglial cells. We thus tested the hypothesis that microglia were proper phagocytes for β-amyloid and performed multiple staining with the use of antibodies directed against either β-amyloid-42, LAMP2, or *iba1* in brain tissues from 6-month-old irradiated and GFP-transplanted mice. As depicted by Figure 6A, β-amyloid-42 and LAMP2 staining were colocalized within GFP-positive microglial cells in vivo. This demonstrates that blood-derived microglia are attempting to clear the amyloid deposits by phagocytosis in vivo. To further confirm these results, cultured microglial cells were treated with β-amyloid-42 and subsequently observed by confocal microscopy. Exogenous Cy3-conjugated β-amyloid was found to be localized inside the cultured microglia (Figure 6B), further supporting our in vivo observations. Therefore, microglia can clear β-amyloid by phagocytosis both in vivo and in vitro.

Discussion

It is generally accepted that the immune system is involved in the etiology of Alzheimer's disease. This idea comes from many reports demonstrating that amyloid plaques are often surrounded by microglial cells (Dickson et al., 1988; Haga et al., 1989; Itagaki et al., 1989; Perlmutter et al., 1992; Sheng et al., 1997; Frautschy et al., 1998; Wegiel et al., 2001, 2003, 2004) and the fact that cultured microglial cells react to β-amyloid by producing high levels of inflammatory cytokines, such as IL-1β, TNF-α, and IL-6, among others (Kim and de Vellis, 2005; Walker and Lue, 2005). However, much less data have been obtained regarding the reactivity of microglia to β-amyloid in vivo. In fact, due to the in vivo data published to date, microglial cells have often been thought to be unable to penetrate the core of amyloid plaques (Wegiel et al., 2001, 2003, 2004). These data and the failure to demonstrate that microglial cells are able to phagocytose β-amyloid have led to the assumption that the brain's resident macrophages promote the development of the disease because they produce cytotoxic elements and are unable to clear the β-amyloid deposits. On the other hand, few studies have

demonstrated that an immune response in the CNS may be beneficial to the organism because it reduces the amount of amyloid deposition (Rogers et al., 2002; Malm et al., 2005). Moreover, it has been recently published that NSAIDs delay the progression of AD (Stewart et al., 1997; Anthony et al., 2000; in t' Veld et al., 2001; Yip et al., 2005), whereas other studies demonstrate that NSAID treatments increase the amount of β-amyloid found in the brain. Therefore, the goal of the present study was to determine the nature of the role that microglia play in the development of Alzheimer's disease.

We have recently shown that circulating monocytes are able to infiltrate the CNS parenchyma and differentiate into microglial cells (Simard and Rivest, 2004a). It has also been demonstrated that these cells are preferentially attracted to damaged areas of the brain (Tzeng and Wu, 1999; Kaur et al., 2001; Priller et al., 2001). Interestingly, many reports suggest that activated microglia promote neuroprotection rather than neurodegeneration (Arnett et al., 2001; Mason et al., 2001; Simard and Rivest, 2004b). We thus hypothesized that most of the microglial cells found closely associated with amyloid plaques are newly differentiated blood-derived microglia and that they serve to slow the progression of AD by removing the β-amyloid found in senile plaques. We first compared the properties of amyloid plaques and associated microglial cells in APP_{Swe}/PS1 mice with those of the well-established single-mutant line (APP_{Swe}) and found that they were both very similar in all aspects except that the double-transgenic line developed plaques at a younger age. Amyloid deposits in these animals are similar to those found in human subjects with Alzheimer's disease; therefore, they are a suitable animal model to study this aspect of the disease.

We next asked whether a portion or all of these plaque-associated microglia were blood-derived cells. We created chimeric mice by irradiating APP_{Swe}/PS1 animals and transplanting GFP-expressing bone marrow cells into their bloodstreams. When tissue sections were stained with either Congo red or anti-β-amyloid-42 antibody, it became clear to us that many of the microglia that are in contact with amyloid deposits are indeed of bone marrow origin. Quantitative analyses of the tissues at different ages demonstrated that the infiltration of these cells occurs mostly after the age of 5 months, which is after the onset of the disease, as plaque formation is already taking place. Prior to this age, the vast majority of plaque-associated microglia are resident parenchymal cells.

According to previous studies, β-amyloid-40/42 are the predominant and most toxic forms in amyloid plaques (Nussbaum and Ellis, 2003). We thus tested the ability of different β-amyloid isoforms to attract blood-derived cells. We found that only the β-amyloid-40/42 isoforms were able to cause the infiltration of blood-derived microglia. Moreover, β-amyloid-42 was able to induce the expression of inflammatory genes such as TLR2, IL-1β, and MCP-1, whereas the 31 and 57 amino acid β-amyloid isoforms did not have an effect. The proteins were injected shortly after their solubilization; thus they were likely in monomeric forms, possibly with a percentage of the protein already forming fibrils. However, the physical state of the protein is likely modified once it is in an in vivo environment. Consequently, our study cannot differentiate between the effects of the different physical states of β-amyloid. We then looked at the expression levels of inflammatory genes in our transgenic animals. Interestingly, MCP-1 expression was not detected in significant levels until the age of 9 months in APP695/PS1 animals. As it seems that blood-derived microglia are less abundant in 9-month-old animals, it is tempting to propose that cells in the brains of older mice are trying to compensate for the diminished infiltration by substantially increasing the mRNA expression of this chemokine.

We also found that TLR2 and IL-1β were induced by cells in the vicinity of the amyloid plaques in the APP_{Swe}/PS1 model, which supports gene expression patterns observed in human studies (Kim and de Vellis, 2005; Walker and Lue, 2005). Though TNF-α expression is increased in cultured microglial cells stimulated with β-amyloid (Kim and de Vellis, 2005), this cytokine transcript was not upregulated in our transgenic animals or after β-amyloid injections in wild-type mice. Indeed, the immune response in these animals is not the typical inflammatory response that is observed in many other models of neurodegeneration or acute neurotoxicity. It therefore seems unlikely that inflammation is the direct cause of neuronal dysfunction in this model of AD. The precise role of IL-1β in the development of the disease is still unknown; however, it is quite likely that IL-1β acts as a signal to induce phagocytosis of β-amyloid by microglial cells. If this were truly the case, one would propose that blood-derived microglia were beneficial to the diseased CNS.

In order to test this hypothesis, we infused ganciclovir for 28 days into the lateral ventricles of APP_{Swe}/PS1 animals that were crossed with transgenic animals harboring the TK gene under the control of the CD11b promoter. The drug had to be delivered locally, because animals submitted to daily systemic injections of ganciclovir die after only 10 days of treatment. Nonetheless, undifferentiated monocytes were exposed to the drug with our delivery method, and because they undergo cell-cycle division prior to infiltrating the plaques, these cells would be eliminated before becoming fully differentiated microglia. To confirm the efficiency of our treatment, we immunohistochemically stained tissues from our ganciclovir- and saline-treated animals for MHC-II protein and observed that this protein was only detected near plaques of saline-treated animals (Figure S1). Only newly differentiated bone marrow-derived microglia express components required for antigen presentation (Simard and Rivest, 2004a), suggesting that ganciclovir treatment effectively blocked the infiltration of blood-derived cells. Moreover, our treatment method partially inhibited the increased IL-1β and TLR2 expression that normally accompanies the disease, whereas MCP-1 expression was higher in ganciclovir-treated animals. The latter finding suggests that resident cells in the brains of these animals were attempting to compensate for the lack of infiltration by increasing the expression of the chemoattractant molecule. Finally, two different paradigms of CNS trauma (stab injury and hypoglossal nerve axotomy) demonstrated that treatment of CD11b-TK mice with ganciclovir results in a robust reduction in the quantity of proliferating microglia and the microglial cell population in these mice can also gradually recover

from the ablation of proliferating cells upon cessation of ganciclovir treatment (Gowing et al., 2006).We are therefore confident that our method of drug delivery successfully prevented the infiltration of new microglial cells adjacent and within the plaques.

Another group has recently created CD11b/TK animals and utilized these mice to study the role of microglia in experimental autoimmune encephalomyelitis (Heppner et al., 2005). These authors presented the CD11b/TK mice as a model of microglial paralysis rather than inhibition of proliferating microglia. To the contrary, our mouse model does not have inhibition of parenchymal microglia, but rather has a depletion of newly differentiated bone marrow-derived microglia. This was determined by various approaches, and the most reliable one was the injection of lipopolysaccharide (LPS) directly into the CNS of ganciclovir- and saline-treated TK animals (see Figure S2) to trigger proinflammatory signaling in microglia (Nadeau and Rivest, 2002). These data clearly show that proinflammatory signaling is functional in our CD11b/TK mice, and thus only newly differentiated microglia are being targeted by the drug. This rapid inflammatory reaction to LPS is only taking place in resident microglial cells, not in infiltrating monocytes. We can therefore conclude that we have specifically inhibited the recruitment of blood-derived microglia and not the activation of resident microglia.

Quantitative analysis of our tissues showed that ganciclovir treatment increased the size and number of amyloid plaques when compared to their age-matched saline counterparts. Moreover, the levels of cytokine expression detected in animals that received the drug were lower than animals treated with saline; therefore, the drug was able to attenuate the immune response normally seen in APP_{Swe}/PS1 animals. The facts that GFP^+ cells were more prevalent in 6-month-old animals and that ganciclovir treatment only had an effect at this specific age further demonstrate that our treatment method was effective at blocking the infiltration of monocytic cells. These data and those showing that resident microglial cells were still present in the vicinity of the plaques of ganciclovir-treated animals suggest that newly differentiated microglial cells originating from the blood are able to remove β-amyloid from the extracellular environment, whereas resident microglia are ineffective at β-amyloid phagocytosis. Interestingly, the number and size of amyloid plaques seemed to be lower in 6-month-old saline-treated animals, whereas expression levels of IL-1β and TLR2 seemed higher when compared to untreated transgenic animals (please compare Figure 2C with Figure 5C, and Figure 4C with Figure 5D). These results have a few implications: first, an increased immune response in the brain reduces the amounts of β-amyloid deposits, and second, removing the presence of blood-derived microglial cells completely blocks the positive effects of inflammation in these brains. The first implication is supported by previous studies showing that microglial cell activation by LPS lowers the β-amyloid burden in the hippocampus (Malm et al., 2005). However, here we show that blood-derived microglial cells are able to clear β-amyloid deposits or to prevent their formation.

It has previously been suggested that microglial cells are unable to phagocytose β-amyloid in vivo (Walker and Lue, 2005). Conversely, we observed in our initial findings that microglial cell ramifications often seem to penetrate toward the center of the amyloid deposits with the single-mutant transgenic line (APP_{Swe} mutation). Furthermore, Congo red staining was often seen within cytoplasmic microglial cell structures (see Movie S2). These data suggest that microglial cells may indeed be able to clear β-amyloid deposits by phagocytosis. We found that β-amyloid-42 and lysosomes colocalized in nearly all GFP-positive microglia, whereas the majority non-GFP microglia did not have intracellular β-amyloid-42. This finding and the fact that large plaques in the later stages of the disease, such as those often obtained from human samples, contain fewer blood-derived microglia may explain reports of human studies demonstrating a lack of β-amyloid phagocytosis by microglial cells (Walker and Lue, 2005).

Some studies have proposed that microglia contribute to the deposition of β-amyloid by concentrating the soluble protein and releasing it into the cellular environment once it dies by apoptosis or by producing the protein itself (Wegiel et al., 2001, 2003, 2004), though these studies base their conclusions on many assumptions. However, it must be noted that these studies do not distinguish between resident and blood-derived microglial cells. It is possible that one of these cells favors plaque formation, while the other serves to prevent or clear amyloid deposits. Three major results provided by the present study support this hypothesis. First, every plaque observed in our study was accompanied by at least one type of microglial cell, though our analyses demonstrate that blood-derived microglia are only present in senile plaques that have attained a certain size after a certain age, since many of the smaller plaques in the 4- to 5-month-old animals were not associated with GFP^+ cells. This suggests that resident microglia are present at the onset of plaque formation and hence may play a role in this process, whereas blood-derived microglia appear at later stages of the disease and may therefore be attempting to clear the senile plaques. Second, the amount of blood-derived microglia in contact with amyloid plaques seems to slightly decrease, while resident microglia are found in greater numbers at 9 months of age, which coincides with the time when the most significant increase in amyloid deposition occurs. Finally, plaque size and number were much lower in animals treated with saline solution, whereas inhibition of bone marrow-derived microglia substantially increased the presence of amyloid plaques.

In conclusion, we demonstrate that blood-derived microglial cells that are associated with amyloid plaques are able to prevent the formation or eliminate the presence of amyloid deposits in mice that develop the major hallmark of AD. We also show that these cells are specifically attracted to β-amyloid in vivo and that they participate in the elimination of this protein by phagocytosis. The fact that newly recruited microglia are more efficient immune cells compared to their resident counterparts is clearly a beneficial mechanism in restricting disease progression. A novel strategy to target and improve such a process toward β-amyloid deposits could lead to the elimination of toxic senile plaques by bone marrow stem cells in AD.

Experimental Procedures

Animals

Transgenic animals harboring the human presenelin 1 (A246E variant) and a chimeric mouse/human β-amyloid precursor protein (APP_{Swe}) were obtained from The Jackson Laboratory [B6C3-Tg(APP695)3Dbo Tg(PSEN1)5Dbo/J; The Jackson Laboratory, Bar harbor, ME]. Hemizygous transgenic mice expressing green fluorescent protein (GFP) under control of the chicken β-actin promoter and cytomegalovirus enhancer were initially obtained from the same vendor. Transgenic animals that express the thymidine kinase (TK) protein specifically in cells of monocytic lineage were generated with the use of standard molecular biology techniques. Briefly, HSV-1 TKmt-30 (TKmt-30) DNA constructs under the control of the human CD11b promoter were created. The CD11b promoter region was amplified by PCR from human genomic DNA using Vent DNA polymerase (NEB, Beverly, MA). The following PCR conditions were used: 94ºC for 4 min, 34 cycles (94ºC for 30 s, 62ºC for 30 s., 72ºC for 2 min) 72ºC for 10 min. The 5′ primer (5′-CCCAAG CTTGGGGGTTCAAGTGATTCTGCTGC-3′) hybridized ≈ 1.7 kb upstream from the main initiation site. The 3′ primer (3′-CGGGATCCC GAGAAACCTGGAGGTG AACC-5′) hybridized 15 bases upstream from the initiation ATG. HindIII and BamHI restriction sites were added to the 5′ and 3′ primers, respectively, for orientation cloning. The PCR products were then subcloned in pBluescript SK+ (Stratagene, La Jolla, CA). The Pet23d vector containing TKmt-30 (a gift from Dr. M. Black, University of Washington) was digested with NcoI to excise a 1.4 kb fragment containing the coding sequence of the TKmt-30 gene (1.1 kb). The TKmt-30 gene was cloned into the BamH1 site of the CD11b pBluescript SK+ vector. A 2.9 kb DNA HindIII and XbaI fragment containing the fusion CD11b-TKmt-30 gene was purified using β-agarose (NEB, Beverly, MA) and then microinjected into one-cell mouse embryos of C57BL/6 genetic background according to standard procedures (Brinster et al., 1981).

The genomic integration of the transgene was confirmed by Southern blot analysis from mouse-tail DNA. An 800 bp TKmt-30 probe was generated by digestion of CD11b- TKmt-30 vector with EcoRV and BssHII. This probe detected a 1.4 kb band corresponding to the TKmt-30 transgene with digestion of mouse genomic DNA by NcoI. Once transgenic lines were established, mice were genotyped by PCR with TAQ DNA polymerase (Amersham, Piscataway, NJ) in 17 mM $MgCl_2$ PCR buffer with the following primers: 5′-CCCCTGCCATCAACACGCGTCTGC and 5′-CGGCGTCGGTCACGG CATAAGGC (position 12–35 and 412–390, respectively). The PCR conditions were as follows: 94ºC for 2 min, 34 cycles (94ºC for 30 s, 55ºC for 30 s, 72ºC for 30 s) 72ºC for 10 min.

These animals were then crossed with the APP695/PSEN1 animals to generate triple-transgenic animals (subsequently named APP-TK animals). Colonies for each strain were maintained in a C57BL/6J background. All animals were acclimated to standard laboratory conditions (14 hr light, 10 hr dark cycle; lights on at 06:00 and off at 20:00 hr) with free access to rodent chow and water. GFP mice were used as cell donors at 4–6 months of age. All protocols were conducted according to the Canadian Council on Animal Care guidelines, as administered by the Laval University Animal Welfare Committee.

Irradiation and Bone Marrow Transplantation

A group of APP_{Swe}/PS1 mice were exposed to 10 gray total-body irradiation using a cobalt-60 source (Theratron-780 model, MDS Nordion, Ottawa, ON, Canada). A few hours later, the animals were injected via a tail vein with $\sim 5 \times 10^6$ bone marrow cells freshly collected from GFP mice. The cells were aseptically harvested by flushing femurs with Dulbecco's PBS containing 2% fetal bovine serum (DPBS-FBS). The samples were combined, filtered through a 40 μm nylon mesh, centrifuged, and passed through a 25 ga needle. Recovered cells were resuspended in DPBS at a concentration of 5×10^6 viable nucleated cells per 200 μl. Irradiated mice transplanted with this suspension were housed in autoclaved cages and treated with antibiotics (0.2 mg trimethoprim and 1 mg sulfamethoxazole/ml of drinking water given for 7 days before and 2 weeks after irradiation). Animals were sacrificed 2–7 months after transplantation.

Intracerebral Injections

Animals were anesthetized with isofluorane, and the site of injection was stereotaxically reached (David Kopf Instruments, Tujunga, CA). For the acute intrahippocampal injections of β-amyloid peptides, the coordinates from the bregma were +2 mm anteroposterior, −2 mm lateral, and −2.3 mm dorsoventral. One microliter of solution containing either 0.9% NaCl or recombinant β-amyloid-31 (1 mg/ml; rPeptide, Athens, GA), β-amyloid-40 (1 mg/ml; Bachem Bioscience Inc., King of Prussia, PA), β-amyloid-42 (1 mg/ml; Bachem Bioscience Inc.), β-amyloid-57 (1 mg/ml; rPeptide), or lipopolysaccharide (LPS 2.5 mg/ml; Sigma Aldrich) was delivered over a period of 2 min. All of the β-amyloid injections were performed within a few hours following solubilization of the drug. The mice then received a 1 ml dose of Ringer's lactate (Abbott Laboratories, Saint-Laurent, Canada) and were housed up to four animals per cage. The animals were then sacrificed at different time points (6, 12, 24, 72, or 168 hr postinjection).

For the chronic intracerebroventricular injections of ganciclovir, the coordinates from the bregma were +0.1 mm anteroposterior, −1 mm lateral, and −3 mm dorsoventral. The guide cannula (Alzet Brain infusion kit III 1–3 mm, Durect Corporation, Cupertino, CA) was secured with screws and cranioplastic cement (Cranioplastic powder, Plastic One Inc., Roanoke, VA; Dentsply repair material, Dentsply International, York, PA). Approximately 40 hr prior to the surgeries, the Alzet pumps (0.25 μL/hr, 28 day pumps, Durect Corporation) were filled with either a solution containing 0.9% saline and 0.04% hydrogen chloride (carrier solution) or a solution containing 1 mg/ml ganciclovir (Cytovene; RocheDiagnostics, Laval, QC, Canada) diluted in carrier solution. The pumps were then incubated in a saline solution at 37ºC until the time of surgery, in order to ensure that drug delivery initiates immediately after implantation. The animals were then housed individually and were sacrificed 28 days following the surgery. The pumps were manually tested to verify that the canula was not blocked and that the drug was delivered throughout the implantation period.

To collect the brain tissues in all experiments described above, mice were deeply anesthetized via an i.p. injection of a mixture of ketamine hydrochloride and xylazine, and then rapidly perfused transcardially with 0.9% saline, followed by 4% paraformaldehyde/3.8% borax in sodium phosphate buffer (pH 9 at 4ºC). Brains were rapidly removed from the skulls, postfixed overnight, and then placed in a solution containing 10% sucrose diluted in 4% paraformaldehyde/3.8% borax buffer (pH 9) overnight at 4ºC. The frozen brains were mounted on a microtome (Reichert-Jung, Cambridge Instruments Company, Deerfield, IL), frozen with dry ice, and cut into 25 μm coronal sections from the olfactory bulb to the end of the medulla. The slices were collected in a cold cryoprotectant solution (0.05 M sodium phosphate buffer, pH 7.3, 30% ethylene glycol, 20% glycerol) and stored at −20ºC.

Immunohistochemistry

Free-floating sections (25 μm thick) were incubated for 30 min in KPBS containing 4% goat serum, 1% BSA, and 0.4% Triton X-100. Using the same buffer solution, the sections were then incubated for 90 min in primary Ab (polyclonal rabbit anti-ionized calcium binding adaptor molecule 1 [*iba1*], 1:2000, Wako Chemicals, Richmond, VA; monoclonal mouse anti-β-$amyloid_{1-42}$, 1:500, Vector Laboratories, Inc., Burlingame, CA; polyclonal rabbit anti-green fluorescent protein [GFP], 1:2000, Molecular Probes, Eugene, OR; monoclonal rat anti-LAMP2 1:500, Developmental Studies Hybridoma Bank, University of Iowa, Iowa City, IA; monoclonal mouse anti-MHC class II $I\text{-}A^b$ 1:500, Cederlane, Hornby, ON, Canada) at room temperature. The sections were then rinsed four times for 5 min in KPBS, followed by a 90 min incubation in fluorochrome- or biotin-conjugated goat secondary Ab (anti-rabbit Alexa-488, 1:1000, Molecular Probes; anti-rabbit Cy5, 1:1000, Jackson ImmunoResearch Laboratories Inc., West Grove, PA; anti-mouse Cy3, 1:500, Jackson ImmunoResearch; anti-mouse AMCA, 1:500, Jackson ImmunoResearch; anti-mouse IgM 1:1000, Vector Laboratories, Inc.). Sections were then rinsed four times for 5 min in KPBS, mounted onto SuperFrost slides (Fisher Scientific, Nepean, Ontario, Canada), stained with DAPI (2×10^{-4}%; Molecular Probes), and coverslipped with antifade medium composed of 96 mM Tris-Hcl, pH 8.0, 24% glycerol, 9.6% polyvinylalcohol, and 2.5% diazabicyclooctane (Sigma). Confocal laser scanning

microscopy was performed with a BX-61 microscope equipped with the Fluoview SV500 imaging software 4.3 (Olympus America Inc, Melville, NY). Confocal images were acquired by sequential scanning using a two-frame Kalman filter and a z-separation of 1 μm. The images were then processed to enhance contrast and sharpness using Adobe Photoshop 7 (Adobe Systems) and were assembled using Adobe Illustrator (Adobe Systems).

In Situ Hybridization

In situ hybridization was performed on every 12th section of the brain, starting from the end of the olfactory bulb to the end of the cortex, using ^{35}S-labeled cRNA probes as described previously (Laflamme and Rivest, 1999; Laflamme et al., 2003; Nadeau and Rivest, 2003).

Estimation by Stereology of Both the Size and Number of the Plaques, and the Number of Infiltrating Microglial Cells Surrounding the Plaques

All quantitative histological analyses were done by an observer who was blind to the treatment status of the material. Overall, 17 APP brains and 32 APP-TK brains were analyzed. Systematically sampled sections (every 12th section through the hippocampus region) were stained with DAPI for nuclei and Congo red for amyloid plaques and immunostained for blood-derived microglial cells with GFP antibody. Using a stereotaxic atlas (Paxinos and Franklin, second edition) as a reference, two slices at −1.70 mm and −3.08 mm from the bregma were analyzed for each brain. The Stereo Investigator software (Microbrightfield, Colchester, VT) was used both to drive a motorized stage (Ludl, Hawthorne, NY) on a dual optical head Nikon C80i microscope and to capture real-time images (1600 × 1200 pixels) from samples with a Microfire CCD color camera (Optronics, Goleta, CA) through a 4× Plan Apochromat objective (NA 0.2) in brightfield mode. The contours of the cortex and hippocampus areas were traced as a virtual overlay on the streamed images with a Cintiq 18S interactive pen display (Wacom, Vancouver, WA). Thereafter, the software sequentially chose counting frames (670 × 500 μm) every 2000 μm in the x axis and every 1000 μm in the y axis while moving automatically the motorized stage into the previously delimited zones in the cortex and the hippocampus. In the selected counting frames, the contour of Congo red-labeled plaques was traced with the interactive pen display by using Stereo Investigator software; the microscope was at this time set with a 40× Plan Apochromat objective (NA 0.95) and a triple-band filter set (DAPI/FITC/TRITC, Chroma Technology, Rockingham, VT) for epifluorescence observations in the three channels simultaneously. The number of labeled cells was estimated by the optical fractionator method in Stereo Investigator software as follows: GFP-immunoreactive cells were counted only if their cell body was in contact with the amyloid plaque and if their nuclei labeled with DAPI laid within the dissector area did not intersect forbidden lines and came into the focus as the optical plane moved through the height of the dissector (20 μm). The guard zone thickness was set to 2 μm. Overall, the sum of the sampling site areas represented around 15% of the total area of the slice. This method of sampling was tested in a pilot experiment to ensure that the estimation of the number of plaques was representative of their total number.

Preparation of Cy3-Labeled Amyloid-β

β-amyloid$_{1-42}$ (Anaspec, San Jose, CA) was dissolved at 1 mg/ml in 50 mM phosphate buffer (pH 7.0–7.3) and conjugated with Cy3 monofunctional dye (Amersham Bioscience, Piscataway, NJ) following the manufacturer's guidelines. Briefly, 5 μl of coupling buffer was thoroughly mixed to 100 μl of the solution of amyloid peptides, the resulting solution was then mixed to the vial of Cy3 reactive dye and incubated 30 min at room temperature with additional mixing every 10 min. Unconjugated dye was separated from the labeled peptides by dialysis overnight in a 3.5 K MWCO Slide-A-Lyzer dialysis cassette (Pierce, Rockford, IL). Fluorescent intensity of dialysed Cy3-labeled Amyloid peptides was measured with a SLM AMINCO Bowman AB2 spectrofluorimeter (Exc: 550 ± 4 nm; Em: 564 ± 4 nm; sensitivity: 835 volts, high-voltage enable) and compared to a nondialysed one (100% of Cy3 dye); only 12.3% of the Cy3 fluorescence was remaining after dialysis. Taking into account that a 1-42 amyloid peptide exposed seven free amino groups for conjugation, 40% of the amyloid peptides could be fully labeled with Cy3 dye, suggesting that the dialysis was complete (no more Cy3-reactive dye than conjugation sites). The solution of Cy3-labeled amyloid peptide was used later as a fluorescent tracer when mixed with nonlabeled amyloid proteins in cell culture medium.

Cell Culture and Immunocytochemistry

BV2 microglial cells (generously provided by Dr. Luc Vallières) were routinely grown in DMEM (Gibco, Invitrogen, Burlington, ON) supplemented with 10% fetal bovine serum (Wisent, St-Bruno, QC), 100 units of penicillin/ml, 100 βg of streptomycin/ml, at pH 7.4 and 37°C in an H_2O-saturated, 5% CO_2 atmosphere. Cells were seed at 10000 cells per well in height-chamber glass slides (Lab-Tek, Nalge Nunc International, Rochester, NY). Two days later, cells were incubated for 1 hr with 25 βg/ml β-amyloid$_{1-42}$ (Anaspec, San Jose, CA) and 2.5 μg/ml of Cy3-labeled β-amyloid$_{1-42}$. Thereafter, cells were rinsed several times with HBSS and then fixed with 4% formaldehyde (pH 7.4) during 15 min at 37°C. Cells were rinsed three times with HBSS. Chambers were removed from the slide, and cells were coverslipped with a polyvinyl alcohol (Sigma-Aldrich) mounting medium containing 2.5% 1,4-diazabicyclo(2,2,2)-octane (Sigma-Aldrich) in buffered glycerol (Sigma-Aldrich).

Confocal Laser Scanning Microscopy for Phagocytosis Experiments

Confocal laser scanning microscopy was performed with a BX-61 microscope equipped with the Fluoview SV500 imaging software 4.3 (Olympus America Inc, Melville, NY), using a 100× Plan-Apochromat oil-immersion objective (NA 1.35) and a 2–3.5× zoom ratio in the region of interest. Cy3-labeled amyloid peptide was excited at 543 nm using an argon-He laser (Melles Griot Laser Group [Carlsbad, CA]) set at 70% of maximum power. Fluorescence emission from Cy3 dye was recorded by photomultipliers with emission filter preset within FV500 software (Red pseudocolor; BA: 560–600 nm). Transmission channel was captured in the same time to delineate the shape of the cells. 0.1 μm confocal z-series were acquired for each observation area and filtered by three-frame Kalman low-speed scans. Acquired z-series images were exported in Imaris Pro Sofware 4.2.0 (Bitplane AG, Zurich, CH).

Tridimensional Reconstructions, Modelings, and Animations

Z-series of the different experiments were imported from the Olympus Fluoview format to the Imaris Pro Software running on a Dell Precision 650 dual Intel Xeon workstation equipped with 4 GB of RAM and a PNY Quadro FX3000G graphic accelerator. Image thresholding and channel pseudocolors were adjusted, and 3D reconstruction was performed in a Surpass Scene as follows: orthogonal view of either the maximum intensity projection (MIP) or the blend projection of the volume of the stacked images were captured, first, channel by channel, and then all the channels together in the Surpass module. Pictures were cropped with Adobe Photoshop CS and thereafter assembled in Adobe Illustrator CS. Modelling of the objects was performed in perspective view, channel by channel; while overlaying carefully with 3D rotations the objects from the original MIP volume with the new isosurfaces generated by advanced Gaussian filter/Threshold level settings. Objects were automatically closed at the border. Light source was set to optimize the 3D rendering effects on the textures wrapping the different objects. Animations were created in two steps. First, movements of the amyloid plaque in 3D were added as key frames in the animation scenario. In a second step, several effects, such as MIP background for volume/blend background for models, zoom in/out, opacity/transparency of specific channels, yellow selection boxes, clipping planes, and ortho slicers were added at specific time points to look inside and around the amyloid plaque and put in evidence the intimate relationships between the plaque and the surrounding microglial cells. High-resolution movies were exported in the .avi file format and then heavily compressed with Microsoft Windows Movie Maker.

Supplemental Data

The Supplemental Data for this article can be found online at http://www.neuron.org/cgi/content/full/49/4/489/DC1/.

Acknowledgments

The Canadian Institutes in Health Research (CIHR) supported this research. A.R.S. is supported by a Ph.D. Studentship from the CIHR. J.-P.J. and S.R. hold a Canadian Research Chair in Neurodegenerative Diseases and Neuroimmunology, respectively. The authors thank Nataly Laflamme, Pierre-Etienne Tremblay, and Eveline Grenier-Hébert for their technical assistance; and Dr. M. Black (Washington State University, Pullman, WA) for the gift of the Pet23d vector containing the HSV-1 TK mutant-30.

Received: September 23, 2005
Revised: December 1, 2005
Accepted: January 6, 2006
Published: February 15, 2006

References

Aisen, P.S., Schafer, K.A., Grundman, M., Pfeiffer, E., Sano, M., Davis, K.L., Farlow, M.R., Jin, S., Thomas, R.G., and Thal, L.J. (2003). Effects of rofecoxib or naproxen vs placebo on Alzheimer disease progression: a randomized controlled trial. JAMA *289*, 2819–2826.

Anthony, J.C., Breitner, J.C., Zandi, P.P., Meyer, M.R., Jurasova, I., Norton, M.C., and Stone, S.V. (2000). Reduced prevalence of AD in users of NSAIDs and H2 receptor antagonists: the Cache County study. Neurology *54*, 2066–2071.

Arnett, H.A., Mason, J., Marino, M., Suzuki, K., Matsushima, G.K., and Ting, J.P. (2001). TNF alpha promotes proliferation of oligodendrocyte progenitors and remyelination. Nat. Neurosci. *4*, 1116–1122.

Brinster, R.L., Chen, H.Y., and Trumbauer, M.E. (1981). Mouse oocytes transcribe injected Xenopus 5S RNA gene. Science *211*, 396–398.

Dickson, D.W., Farlo, J., Davies, P., Crystal, H., Fuld, P., and Yen, S.H. (1988). Alzheimer's disease. A double-labeling immunohistochemical study of senile plaques. Am. J. Pathol. *132*, 86–101.

Frautschy, S.A., Yang, F., Irrizarry, M., Hyman, B., Saido, T.C., Hsiao, K., and Cole, G.M. (1998). Microglial response to amyloid plaques in APPsw transgenic mice. Am. J. Pathol. *152*, 307–317.

Giulian, D., Haverkamp, L.J., Yu, J.H., Karshin, W., Tom, D., Li, J., Kirkpatrick, J., Kuo, L.M., and Roher, A.E. (1996). Specific domains of beta-amyloid from Alzheimer plaque elicit neuron killing in human microglia. J. Neurosci. *16*, 6021–6037.

Gowing, G., Vallieres, L., and Julien, J.P. (2006). Mouse model for ablation of proliferating microgliain acute CNS injuries. Glia *53*, 331–337.

Haga, S., Akai, K., and Ishii, T. (1989). Demonstration of microglial cells in and around senile (neuritic) plaques in the Alzheimer brain. An immunohistochemical study using a novel monoclonal antibody. Acta Neuropathol. (Berl.) *77*, 569–575.

Heppner, F.L., Greter, M., Marino, D., Falsig, J., Raivich, G., Hovelmeyer, N., Waisman, A., Rulicke, T., Prinz, M., Priller, J., et al. (2005). Experimental autoimmune encephalomyelitis repressed by microglial paralysis. Nat. Med. *11*, 146–152.

Hess, D.C., Abe, T., Hill, W.D., Studdard, A.M., Carothers, J., Masuya, M., Fleming, P.A., Drake, C.J., and Ogawa, M. (2004). Hematopoietic origin of microglial and perivascular cells in brain. Exp. Neurol. *186*, 134–144.

in t' Veld, B.A., Ruitenberg, A., Hofman, A., Launer, L.J., van Duijn, C.M., Stijnen, T., Breteler, M.M., and Stricker, B.H. (2001). Nonsteroidal antiinflammatory drugs and the risk of Alzheimer's disease. N. Engl. J. Med. *345*, 1515–1521.

Itagaki, S., McGeer, P.L., Akiyama, H., Zhu, S., and Selkoe, D. (1989). Relationship of microglia and astrocytes to amyloid deposits of Alzheimer disease. J. Neuroimmunol. *24*, 173–182.

Kaur, C., Hao, A.J., Wu, C.H., and Ling, E.A. (2001). Origin of microglia. Microsc. Res. Tech. *54*, 2–9.

Kim, S.U., and de Vellis, J. (2005). Microglia in health and disease. J. Neurosci. Res. *81*, 302–313.

Kukar, T., Murphy, M.P., Eriksen, J.L., Sagi, S.A., Weggen, S., Smith, T.E., Ladd, T., Khan, M.A., Kache, R., Beard, J., et al. (2005). Diverse compounds mimic Alzheimer disease-causing mutations by augmenting Abeta42 production. Nat. Med. *11*, 545–550.

Laflamme, N., and Rivest, S. (1999). Effects of systemic immunogenic insults and circulating proinflammatory cytokines on the transcription of the inhibitory factor kappaB alpha within specific cellular populations of the rat brain. J. Neurochem. *73*, 309–321.

Laflamme, N., Echchannaoui, H., Landmann, R., and Rivest, S. (2003). Cooperation between toll-like receptor 2 and 4 in the brain of mice challenged with cell wall components derived from gram-negative and gram-positive bacteria. Eur. J. Immunol. *33*, 1127–1138.

Liu, Y., Walter, S., Stagi, M., Cherny, D., Letiembre, M., Schulz-Schaeffer, W., Heine, H., Penke, B., Neumann, H., and Fassbender, K. (2005). LPS receptor (CD14): a receptor for phagocytosis of Alzheimer's amyloid peptide. Brain *128*, 1778–1789.

Malm, T.M., Koistinaho, M., Parepalo, M., Vatanen, T., Ooka, A., Karlsson, S., and Koistinaho, J. (2005). Bone-marrow-derived cells contribute to the recruitment of microglial cells in response to beta-amyloid deposition in APP/PS1 double transgenic Alzheimer mice. Neurobiol. Dis. *18*, 134–142.

Mason, J.L., Suzuki, K., Chaplin, D.D., and Matsushima, G.K. (2001). Interleukin-1beta promotes repair of the CNS. J. Neurosci. *21*, 7046–7052.

Nadeau, S., and Rivest, S. (2002). Endotoxemia prevents the cerebral inflammatory wave induced by intraparenchymal lipopolysaccharide injection: role of glucocorticoids and CD14. J. Immunol. *169*, 3370–3381.

Nadeau, S., and Rivest, S. (2003). Glucocorticoids play a fundamental role in protecting the brain during innate immune response. J. Neurosci. *23*, 5536–5544.

Nguyen, M.D., Julien, J.P., and Rivest, S. (2002). Innate immunity: the missing link in neuroprotection and neurodegeneration? Nat. Rev. Neurosci. *3*, 216–227.

Nussbaum, R.L., and Ellis, C.E. (2003). Alzheimer's disease and Parkinson's disease. N. Engl. J. Med. *348*, 1356–1364.

Perlmutter, L.S., Scott, S.A., Barron, E., and Chui, H.C. (1992). MHC class II-positive microglia in human brain: association with Alzheimer lesions. J. Neurosci. Res. *33*, 549–558.

Priller, J., Flugel, A., Wehner, T., Boentert, M., Haas, C.A., Prinz, M., Fernandez-Klett, F., Prass, K., Bechmann, I., de Boer, B.A., et al. (2001). Targeting gene-modified hematopoietic cells to the central nervous system: use of green fluorescent protein uncovers microglial engraftment. Nat. Med. *7*, 1356–1361.

Rogers, J., and Lue, L.F. (2001). Microglial chemotaxis, activation, and phagocytosis of amyloid beta-peptide as linked phenomena in Alzheimer's disease. Neurochem. Int. *39*, 333–340.

Rogers, J., Strohmeyer, R., Kovelowski, C.J., and Li, R. (2002). Microglia and inflammatory mechanisms in the clearance of amyloid beta peptide. Glia *40*, 260–269.

Sheng, J.G., Mrak, R.E., and Griffin, W.S. (1997). Neuritic plaque evolution in Alzheimer's disease is accompanied by transition of activated microglia from primed to enlarged to phagocytic forms. Acta Neuropathol. (Berl.) *94*, 1–5.

Simard, A.R., and Rivest, S. (2004a). Bone marrow stem cells have the ability to populate the entire central nervous system into fully differentiated parenchymal microglia. FASEB J. *18*, 998–1000.

Simard, A.R., and Rivest, S. (2004b). Role of inflammation in the neurobiology of stem cells. Neuroreport *15*, 2305–2310.

Stewart, W.F., Kawas, C., Corrada, M., and Metter, E.J. (1997). Risk of Alzheimer's disease and duration of NSAID use. Neurology *48*, 626–632.

Turrin, N.P., and Rivest, S. (2006). Tumor necrosis factor alpha but not interleukin 1beta mediates neuroprotection in response to acute nitric oxide excitotoxicity. J. Neurosci. *26*, 143–151.

Tzeng, S.F., and Wu, J.P. (1999). Responses of microglia and neural progenitors to mechanical brain injury. Neuroreport *10*, 2287–2292.

Walker, D.G., and Lue, L.F. (2005). Investigations with cultured human microglia on pathogenic mechanisms of Alzheimer's disease and other neurodegenerative diseases. J. Neurosci. Res. *81*, 412–425.

Wegiel, J., Wang, K.C., Imaki, H., Rubenstein, R., Wronska, A., Osuchowski, M., Lipinski, W.J., Walker, L.C., and LeVine, H. (2001). The role of microglial cells and astrocytes in fibrillar plaque evolution in transgenic APP(SW) mice. Neurobiol. Aging *22*, 49–61.

Wegiel, J., Imaki, H., Wang, K.C., Wronska, A., Osuchowski, M., and Rubenstein, R. (2003). Origin and turnover of microglial cells in fibrillar plaques of APPsw transgenic mice. Acta Neuropathol. (Berl.) *105*, 393–402.

Wegiel, J., Imaki, H., Wang, K.C., and Rubenstein, R. (2004). Cells of monocyte/microglial lineage are involved in both microvessel amyloidosis and fibrillar plaque formation in APPsw tg mice. Brain Res. *1022*, 19–29.

Yip, A.G., Green, R.C., Huyck, M., Cupples, L.A., and Farrer, L.A. (2005). Nonsteroidal anti-inflammatory drug use and Alzheimer's disease risk: the MIRAGE Study. BMC Geriatr. *5*, 2.